

Sensor and Simulation Notes /

Note 431

19 November 1998

Symmetry and SAR Antennas

**Carl E. Baum
Air Force Research Laboratory
Directed Energy Directorate**

Abstract

In polarimetric SAR (synthetic aperture radar) the control of the polarization incident on the target can be an important characteristic in target identification, such as for some targets on or near a flat ground surface. For controlling these polarizations, whether for narrowband CW or for a pulse, symmetry in the transmit/receive antennas and their relation to the earth surface is an important concept. This can be used to give ideal horizontal and vertical polarizations, at least at some target locations, with small deviations from the ideal for nearby target locations.

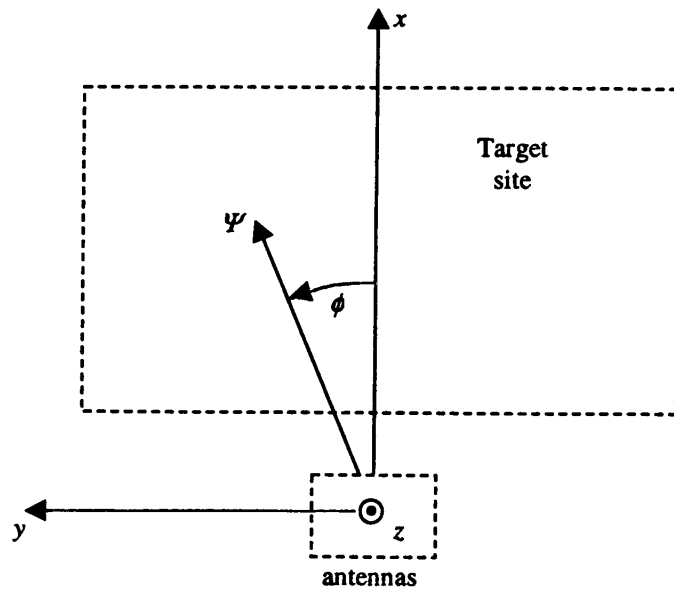
1. Introduction

In synthetic aperture radar (SAR) one moves one or more antennas, say in the y direction in Fig. 1.1, past some target site and takes measurements retaining phase/time information at many positions y . Combining all this data, say in a computer, with correction for distance to each point on the target site gives an image of the target site. The resolution in the y direction (crossrange) is determined by the length of the synthetic aperture so obtained in the y direction. The resolution in the x direction (downrange) is determined by accuracy of round-trip delay (or equivalent phase in frequency domain) between antennas and position in the target site. Note that for present purposes the ground surface S_e is assumed flat and perpendicular to the z axis with the position of the antenna(s) at a constant height h above S_e .

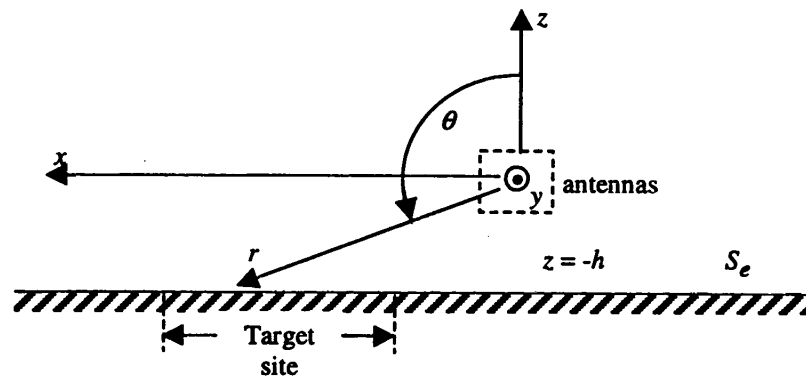
If, instead, one moves the targets past the antennas one has inverse synthetic aperture radar (ISAR). The considerations are fundamentally the same due to relativistic invariance. In the same spirit, let us consider electromagnetic fields at various positions on S_e for a specific antenna position ($\vec{r} = \vec{0}$), instead of moving the antennas and considering a fixed position on the target site. Thereby we will see the variation of the fields for various angular and distance relations of the targets to the antennas.

The SAR can be fully polarimetric with two polarizations for transmit and receive to obtain the full 2×2 scattering matrix for the target referred to some h, v (horizontal, vertical) coordinate system. Referring to Fig. 1.1 horizontal is usually intended to mean parallel to the ground surface S_e with vertical meaning in the vertical plane of incidence, a plane S_ϕ of constant azimuth ϕ . As one varies ϕ and r , however, the polarization of the field from an antenna with fixed orientation (not rotating as it translates) can vary from the ideal, depending on the antenna design. The incident field at S_e is, of course, propagating in the r direction which varies with ϕ and r . The polarization relative to S_ϕ and S_e can also vary depending on the antenna pattern. We would like to control this pattern, particularly for its polarization properties. The amplitude of the incident field in the far field, of course, varies as $1/r$.

Looking ahead, with the $y = 0$ plane designated S_y as a symmetry plane for the antenna(s) and ground, we have pure vertical and horizontal polarization on S_y (also designated by $\phi = 0$). Based on this we can speak of the antenna(s) as operating in "vertical mode" and "horizontal mode" in both transmission and reception. Retaining these labels for ϕ away from 0, we recognize that the polarizations may not be truly vertical and horizontal, respectively, for each mode. We can furthermore observe that a true vertical polarization, meaning parallel (or antiparallel) to $\vec{1}_\theta$, varies depending on the relative location of antenna and target. So as the antenna is moved (in the $\vec{1}_y$ direction) relative to a target, the vertical polarization at the target changes. Similarly, a true horizontal polarization, meaning parallel (or antiparallel) to $\vec{1}_\phi$, varies at a target as the antenna is moved, although it does remain parallel to S_e .



A. Top view



B. Side view: assumed flat (horizontal) ground surface

Fig. 1.1. Coordinates for Antennas and Targets

For some purposes one may wish a horizontal polarization defined by $\vec{1}_y$. However, as we have seen, this cannot be exactly realized except for $\phi = 0$. If this is important one must note that it can only be approximately realized for a restricted range of ϕ around $\phi = 0$. Similarly one may wish that a vertical polarization be parallel to a plane of constant y . This is also limited to ϕ near 0 and/or θ near $\pi/2$ (large Ψ/h).

If the SAR uses a pulse (instead of narrowband CW) [12], this pulse will in general be a function of r (or Ψ) and ϕ on S_e . In particular, the frequency spectrum of the incident field can vary (even in the far field) as a function of the angles (θ and ϕ). This variation with frequency includes polarization as well. Of course, one can use many frequencies instead of a pulse to obtain the same information, and the pattern and polarization questions are similar.

In order to control the antenna pattern and polarization, including for pulses, this paper considers the use of symmetry in the antenna design. Specifically the point symmetry groups (rotations and reflections) [10] are considered. Such symmetry can be applied to the antenna(s) and the resulting incident field. It can also be applied in the presence of the ground surface S_e (thereby including the ground-scattered fields).

One can relax the symmetry requirements somewhat through the concept of partial symmetry [11]. In this case causality gives the result that the signal from the back (negative x) of the antenna reaches the target after the signal (positive x) from the front. For a limited amount of time (the clear time) the fields at the target are the same even with the back portions of the antenna removed. This applies to fast pulses (including those synthesized from many frequencies). Of course, no real antenna is perfect and various errors (hopefully small) will result.

For this analysis we have the coordinates illustrated in Fig. 1.1. Cylindrical (Ψ, ϕ, z) and spherical (r, θ, ϕ) coordinates are related to Cartesian (x, y, z) coordinates via

$$\begin{aligned}
 x &= \Psi \cos(\phi) \quad , \quad y = \Psi \sin(\phi) \\
 \Psi &= r \sin(\theta) \quad , \quad z = r \cos(\theta) \\
 \Psi &= \left[x^2 + y^2 \right]^{\frac{1}{2}} \quad , \quad r = \left[\Psi^2 + z^2 \right]^{\frac{1}{2}} = \left[x^2 + y^2 + z^2 \right]^{\frac{1}{2}}
 \end{aligned}
 \tag{1.1}$$

The associated unit vectors are

$$\begin{aligned}
 \vec{1}_x &= \vec{1}_\Psi \cos(\phi) - \vec{1}_\phi \sin(\phi) \quad , \quad \vec{1}_y = \vec{1}_\Psi \sin(\phi) + \vec{1}_\phi \cos(\phi) \\
 \vec{1}_\Psi &= \vec{1}_x \cos(\phi) + \vec{1}_y \sin(\phi) \quad , \quad \vec{1}_\phi = -\vec{1}_x \sin(\phi) + \vec{1}_y \cos(\phi)
 \end{aligned}$$

$$\begin{aligned}
\vec{1}_r &= \vec{1}_\psi \sin(\theta) + \vec{1}_z \cos(\theta) \\
&= \vec{1}_x \sin(\theta)\cos(\phi) + \vec{1}_y \sin(\theta)\sin(\phi) + \vec{1}_z \cos(\theta) \\
\vec{1}_\theta &= \vec{1}_\psi \cos(\theta) - \vec{1}_z \sin(\theta) \\
&= \vec{1}_x \cos(\theta)\cos(\phi) + \vec{1}_y \cos(\theta)\sin(\phi) - \vec{1}_z \sin(\theta) \\
\vec{1}_\psi &= \vec{1}_r \sin(\theta) + \vec{1}_\theta \cos(\theta) \quad , \quad \vec{1}_z = \vec{1}_r \cos(\theta) - \vec{1}_\theta \sin(\theta)
\end{aligned}
\tag{1.2}$$

These coordinates are related to both the antenna and ground surface $S_e (z = -h)$ as in Fig. 1.1. Later, other coordinates are introduced for special antenna types and orientations. These are rotations of the above coordinates (still centered on the antenna(s)), and are distinguished by subscripts.

2. Target Symmetry

In addition to the antenna(s) some targets of interest on or near the ground surface have important symmetries. In particular if the target is a body of revolution with rotation axis $\vec{1}_a = \vec{1}_z$ with axial symmetry planes (infinitely many), then in the h, v coordinates (true, as discussed in Section 1) there is no cross polarization in the backscattering dyadic [7, 8]. The lack of an h, v component (and hence of a v, h component due to reciprocity) is called the vampire signature.

For this special signature then it is useful to have the horizontal defined by $-\vec{1}_\phi$ and the vertical by $-\vec{1}_\theta$ in the coordinates of Section 1.

3. O_2 Antennas with Respect to the z Axis (True Vertical)

A class of antennas with a high degree of symmetry is described by the O_2 symmetry group (orthogonal in two dimensions). With the axis of revolution $\vec{1}_a$ taken as the z axis, the ground surface S_e and any vertical layering of the assumed isotropic earth fit into this symmetry as well [7]. Another way of designating this symmetry group is $C_{\infty a}$ indicating invariance to all two-dimensional rotations with every axial plane (containing $\vec{1}_a$) a symmetry plane.

As indicated in Fig. 3.1 one can obtain the two polarizations by appropriate antenna designs. The vertical mode (Fig. 3.1A) has current density restricted as

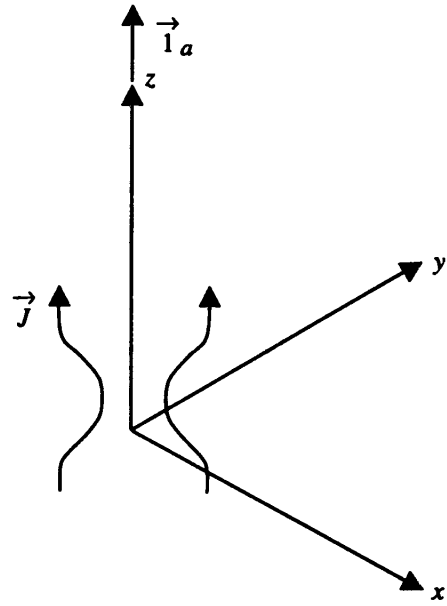
$$\begin{aligned}\vec{J} &= J_{\Psi}(\Psi, z) \vec{1}_{\Psi} + J_z(\Psi, z) \vec{1}_z \\ &= J_r(r, \theta) \vec{1}_r + J_{\theta}(r, \theta) \vec{1}_{\theta}\end{aligned}\tag{3.1}$$

Various antennas such as a circular bicone or thin-wire or ACD (asymptotic conical dipole) [9] coaxial with the z axis have this property. Note that these antenna currents are in transmission. In reception additional currents (orthogonal to the above) are induced in the antenna, but the axially symmetric coupling of signals to/from the antenna only interacts with this basic form in (3.1).

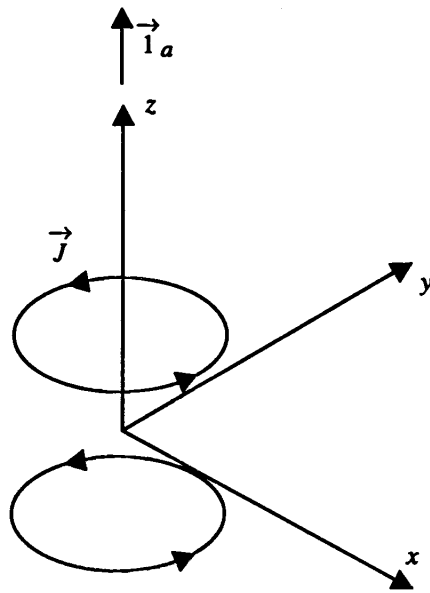
The horizontal mode (Fig. 3.1B) has current density (in transmission) restricted as

$$\vec{J} = J_{\phi}(\Psi, \phi) \vec{1}_{\phi} = J_{\phi}(r, \theta) \vec{1}_{\phi}\tag{3.2}$$

Electrically small circular loops coaxial with the z axis have this property. As the wavelength decreases to become comparable to the loop circumference one needs to take care in enforcing (3.2), say by multiple signal feed points uniformly spaced around the loop circumference. Such techniques have been used in various types of sensors such as the MGL (multigap loop) and others discussed in [9]. In the limit of a large number of such azimuthal, equal-amplitude sources the above ideal divergenceless (zero-charge density) current distribution is achieved. Again in reception other distributions may be induced on the antenna structure, but summing (or averaging) the signals from the azimuthally distributed signal ports gives a response to the desired term as in (3.2).



A. Vertical mode



B. Horizontal mode

Fig. 3.1. Antenna Currents in Transmission with O_2 Symmetry for Two Polarizations

The electromagnetic fields radiated by such antennas have, for the vertical mode, a θ component of the far electric field (including an r component in the near field) and a ϕ component of the magnetic field, all independent of ϕ . In the far field these vary as $1/r$ times a function of θ . This is the ideal type of polarization (for an antenna limited to near $\vec{r} = \vec{0}$) discussed in Section 1. For the horizontal mode the roles of electric and magnetic field are interchanged as compared to the vertical mode, retaining the ideal type of polarization. Again there are the limitations of rotation of $\vec{1}_\theta$ and $\vec{1}_\phi$ as Ψ and ϕ to the target are varied. This variation is minimized for ϕ restricted to near 0 and θ near $\pi/2$ (side looking).

One can impose additional symmetries such as R_z (reflection through the $z = 0$ plane). This gives dihedral symmetry $D_{\infty d}$ [10]. One can design both vertical- and horizontal-mode antennas into a single antenna structure, or have them displaced coaxially along the z axis.

4. O_2 Antennas with Respect to the y Axis (Horizontal in the Direction of Antenna Motion)

Antennas with O_2 symmetry can also be oriented horizontally as indicated in Fig. 4.1. Note now that the symmetry applies only to the incident fields since S_e is now parallel to the rotation axis $\vec{1}_a$ of the antennas. For convenience now we introduce a new set of coordinates, designated by a subscript h with the interchange (rotation) of coordinates as

$$x_h = z, \quad y_h = x, \quad z_h = y \quad (4.1)$$

With this subscript then we have cylindrical and spherical coordinates as in (1.1) and (1.2) referenced to the z_h axis.

Note now that the rotation symmetry makes every plane of constant ϕ_h a symmetry plane. As indicated in Fig. 4.1 we can define an elevation angle at the target by

$$\psi = \phi_h - \frac{\pi}{2} \quad (4.2)$$

Such planes, designated S_ψ are then symmetry planes for the incident field. Every target in the target site is intersected by some S_ψ .

Vertical mode for polarization is now defined by the loop-like currents in Fig. 3.1B with now a subscript h on the z coordinate. The associated electric field for the incident wave now has only a ϕ_h component. This incident electric field is perpendicular to S_ψ and as such has only y_h and z_h components, or x and z components in the original coordinate system. With a z_h (or y) component, the polarization varies as a function only of y_h (or x) on S_e . For small variation of ψ over the target site, this is a small variation of the vertical-mode polarization. The associated incident magnetic field has only a θ_h component. This is not truly horizontal (except for $z_h = 0 = y$). From (1.2) we have

$$\vec{1}_{\theta_h} = \vec{1}_{x_h} \cos(\theta_h) \cos(\phi_h) + \vec{1}_{y_h} \cos(\theta_h) \sin(\phi_h) + \vec{1}_z \sin(\theta_h) \quad (4.3)$$

giving generally all three Cartesian components. For θ_h , near $\pi/2$ and/or ϕ_h near $\pi/2$ (small ψ), however, the true vertical component can be small.

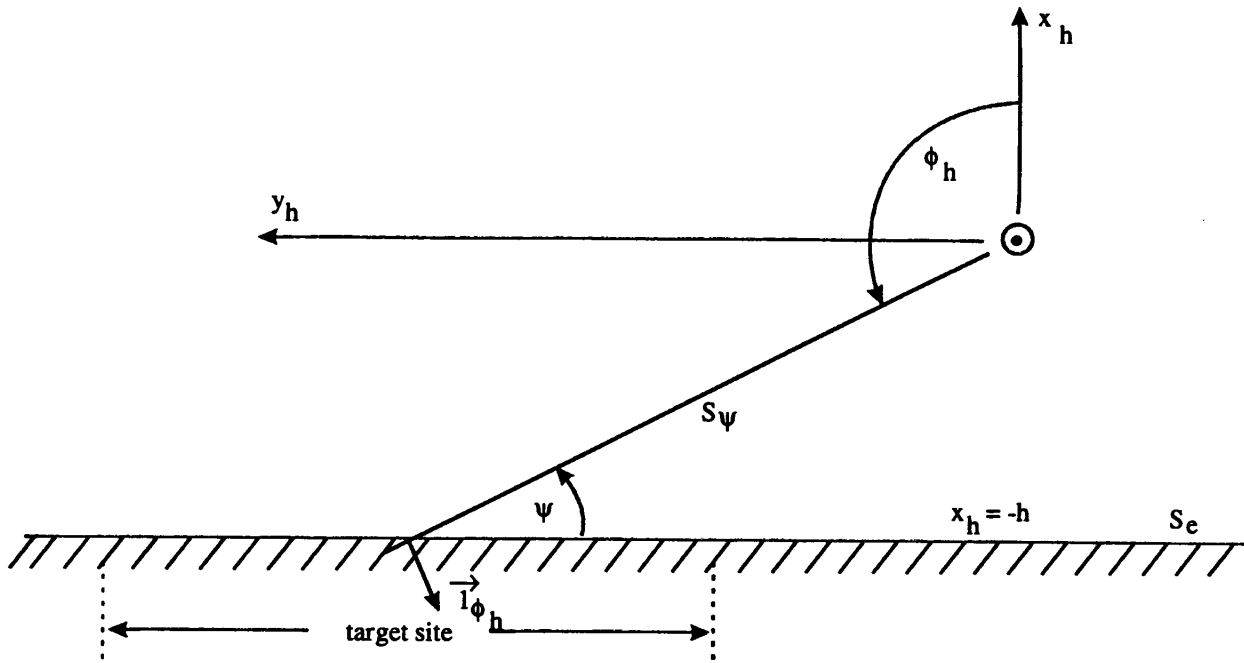


Fig. 4.1. Horizontal O_2 -Symmetry Antennas In Presence of Earth: Side View.

Horizontal mode for polarization is now defined by axial and radial currents in Fig. 3.1A, now with respect to the z_h coordinate. The radiated electric field has a θ_h component while the radiated magnetic field has a ϕ_h component. This merely interchanges the roles of the two components that exist in the vertical mode.

5. R_y Antennas: Vertical Symmetry Plane

A lesser symmetry is that of a single symmetry plane. Figure 5.1 shows the case of a vertical symmetry plane S_y for both the antennas and the ground. The fields are then established as symmetric for vertical mode and antisymmetric for horizontal mode [10]. Symmetric fields have \vec{E} parallel to S_y and \vec{H} perpendicular to S_y on the symmetry plane. Antisymmetric fields have the two field orientations on S_y interchanged from the symmetric case. This assures pure vertical and horizontal polarizations on S_y , and hence along a path on the ground surface S_e given by $(y, z) = (0, -h)$.

Considering vertical mode (symmetric) we have

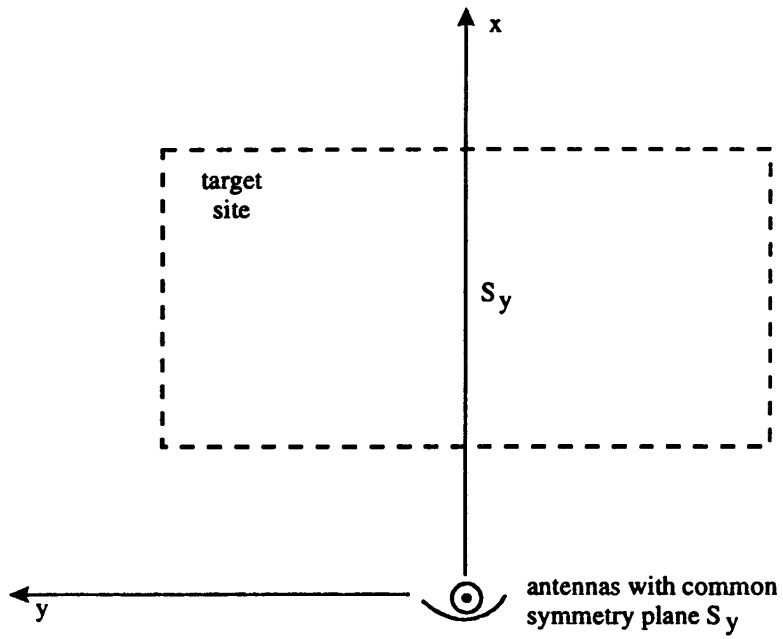
$$\begin{aligned}
 \vec{E}(x, -y, z) &= \overleftrightarrow{R}_y \cdot \vec{E}(x, y, z) \\
 \vec{H}(x, -y, z) &= -\overleftrightarrow{R}_y \cdot \vec{H}(x, y, z) \\
 \overleftrightarrow{R}_y &= \vec{1}_x \vec{1}_x - \vec{1}_y \vec{1}_y + \vec{1}_z \vec{1}_z = \begin{pmatrix} 1 & 0 & 0 \\ 0 & -1 & 0 \\ 0 & 0 & 1 \end{pmatrix} \quad (5.1) \\
 E_y(x, 0, z) &= 0 \\
 H_x(x, 0, z) &= 0 \\
 H_z(x, 0, z) &= 0
 \end{aligned}$$

Expanding the fields in a power (Taylor) series near $y = 0$ we have variation of the fields here as

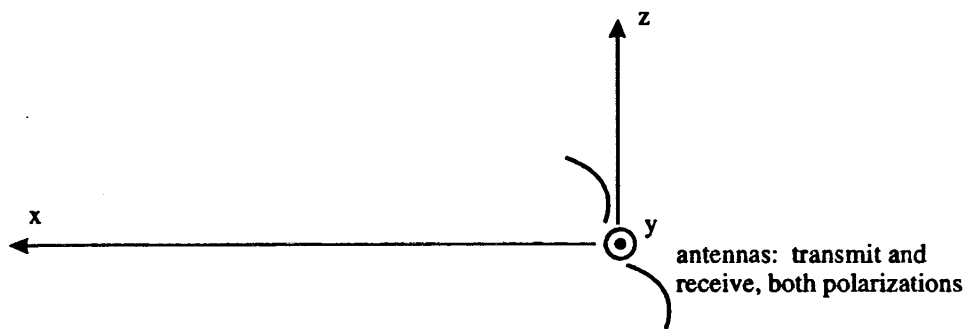
$$\begin{aligned}
 E_y(x, y, z) &: \text{first order in } y \text{ (odd)} \\
 E_x(x, y, z) \text{ and } E_z(x, y, z) &: \text{second order variation from values at } y = 0 \text{ (even)} \\
 H_x(x, y, z) \text{ and } H_z(x, y, z) &: \text{first order in } y \text{ (odd)} \quad (5.2) \\
 H_y(x, y, z) &: \text{second order variation from value at } y = 0 \text{ (even)}
 \end{aligned}$$

So while the fields do not have ideal polarization away from $y = 0$, smooth variation of the fields makes the deviation small and of the form in (5.2) due to the symmetry.

For horizontal mode (antisymmetric) the roles of electric and magnetic fields in (5.1) and (5.2) are simply interchanged. Near $y = 0$ then these have the same small deviations from the ideal polarization.



A. Top view



B. Side view

Fig. 5.1. Antennas with a Common Vertical Symmetry Plane.

Note in fig. 5.1 that for these symmetry results to hold, the horizontal and vertical antennas need not be colocated. They merely need to share the common S_y symmetry plane. However, if they are closely spaced the angles from each to the target will be nearly the same, thereby approximating backscattering.

6. R_0 Antennas: Nearly Horizontal Symmetry Plane

Another choice for a symmetry plane is illustrated in Fig. 6.1. In this case we choose a symmetry plane S_0 which contains the y axis (and is thereby perpendicular to S_y). Instead of being exactly horizontal, let this plane intersect the earth surface S_e somewhere in the middle of the target site. The deviation angle ψ introduced in Section 4 is taken to have the specific value ψ_0 in this case.

Note now that the antennas are symmetric with respect to S_0 . The incident fields are symmetric (horizontal mode) or antisymmetric (vertical mode) with respect to this plane with the symmetry described by a reflection dyadic of the form

$$\begin{aligned} \overleftrightarrow{R}_0 &= \overleftrightarrow{1} - \vec{1}_0 \vec{1}_0, \quad \vec{1}_0 \perp S_0 \\ \overleftrightarrow{1} &= \vec{1}_x \vec{1}_x + \vec{1}_y \vec{1}_y + \vec{1}_z \vec{1}_z \equiv \text{identity} \end{aligned} \tag{6.1}$$

This can be interpreted in terms of the fields in Section 5 by an appropriate rotation of coordinates. Hence, near S_0 the fields have small deviation from being perpendicular or parallel to S_0 .

Since S_0 is not the same as S_e , then the fields are not perpendicular or parallel to S_e , but are nearly so if ψ_0 is small. Furthermore S_0 intersects S_e in the target site along some line of constant x . If, however, ψ_0 is sufficiently small, and the target site is not too extensive in the x direction, then the variation of the elevation angle ψ away from ψ_0 is small and the vertical/horizontal decomposition of the fields over the target site approximately holds.

While Fig. 6.1 illustrates the fields for the vertical mode on a ray on S_y ($y = 0$ plane), one should note that in this case \vec{H} is not in general oriented in the y direction, but is more generally oriented parallel to S_0 . This case is the same for the electric field in horizontal mode.

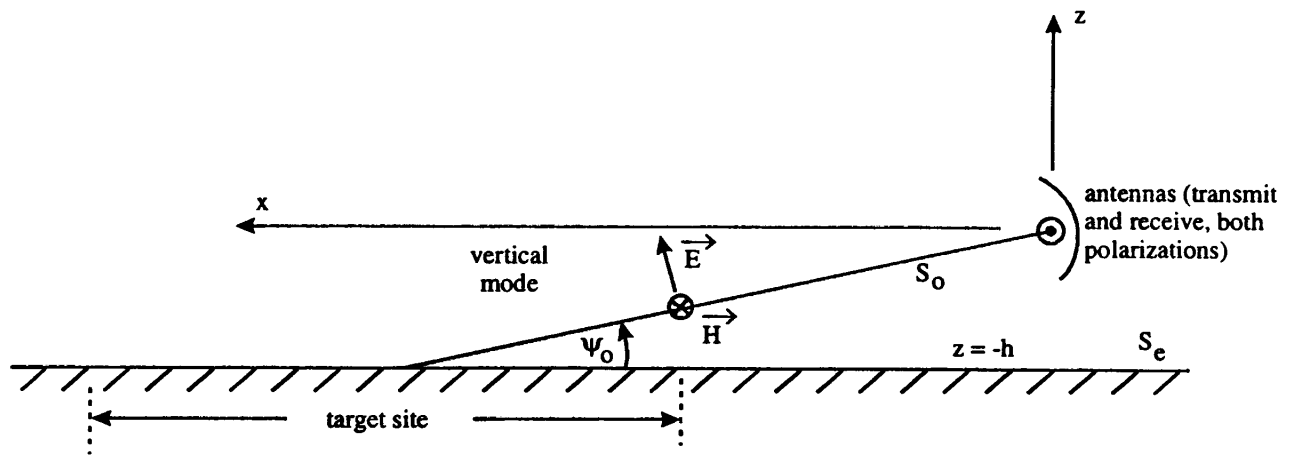


Fig. 6.1. Antennas with a Nearly Horizontal Symmetry Plane.

7. Combined Dipole Antennas

Consider now electrically small (or even larger in special designs) dipoles, electric and magnetic, at the coordinate origin. For this purpose we have the coordinate with subscript c as in Fig. 7.1. the preferred propagation direction (center of pattern) is taken as z_c . The two dipole moments are oriented as

$$\begin{aligned}\vec{p} \cdot \vec{1}_{z_c} &= 0 && \text{(electric-dipole moment)} \\ \vec{m} \cdot \vec{1}_{z_c} &= 0 && \text{(magnetic dipole moment)}\end{aligned}\quad (7.1)$$

Note that the orientation of the (x_c, y_c, z_c) coordinates with respect to the ground surface S_e is not yet specified. These coordinates also are related to each other as in (1.1) and (1.2). Their orientation in terms of the (x, y, z) coordinates in Fig. 1.1 can be specified in various ways to give desired polarizations and directions of propagation.

The special case of interest has the dipole moments at right angles to each other and balanced as [1-6]

$$\begin{aligned}\vec{p} &= p \vec{1}_p, \quad \vec{m} = m \vec{1}_m, \quad p = \frac{m}{c}, \quad c \equiv \text{speed of light} \\ \vec{1}_p \times \vec{1}_m &= \vec{1}_{z_c}, \quad \vec{1}_m \times \vec{1}_{z_c} = \vec{1}_p, \quad \vec{1}_{z_c} \times \vec{1}_p = \vec{1}_m\end{aligned}\quad (7.2)$$

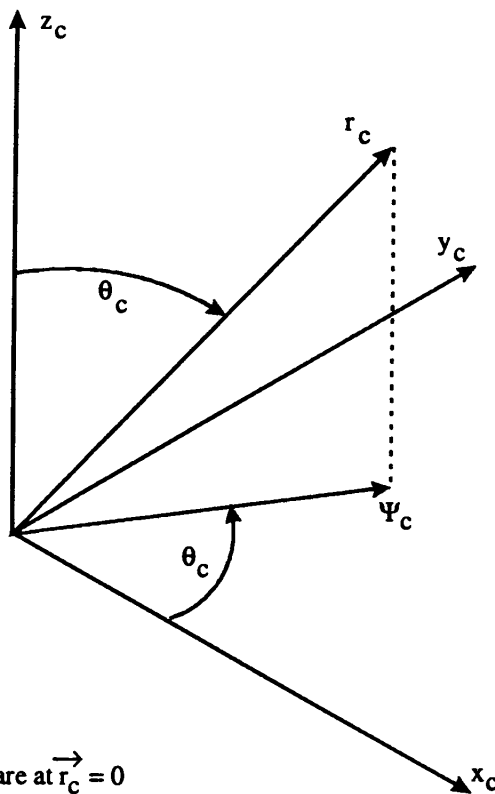
Then on the z_c axis the electric field is polarized parallel (or antiparallel) to $\vec{1}_p$ and the magnetic field similarly to $\vec{1}_m$, and the electric and magnetic field have the ratio Z_0 , the wave impedance of free space, in both near and far fields with Poynting vector in the $\vec{1}_{z_c}$ direction. For convenience now choose

$$\vec{1}_p = \vec{1}_{x_c}, \quad \vec{1}_m = \vec{1}_{y_c}\quad (7.3)$$

consistent with (7.2)

The far fields are given by

$$\begin{aligned}\vec{E}_f(\vec{r}_c, s) &= -\frac{e^{-\gamma r_c}}{4\pi r_c} \mu_0 s^2 \vec{p}(s) \vec{d}_1 \\ \vec{H}_f(\vec{r}_c, s) &= -\frac{e^{-\gamma r_c}}{4\pi r_c Z_0} s^2 \vec{p}(s) \vec{d}_2\end{aligned}$$



Dipole moments \vec{p} and \vec{m} are at $\vec{r}_c = 0$
and parallel to the $x_c y_c$ plane.

Fig. 7.1. Coordinates for Combined Dipole Antennas.

$$\begin{aligned}\vec{d}_1 &= \vec{1}_{r_c} \cdot \vec{1}_{x_c} - \vec{1}_{r_c} \times \vec{1}_{y_c} \\ \vec{d}_2 &\equiv \vec{1}_{r_c} \times \vec{1}_{x_c} + \vec{1}_{r_c} \cdot \vec{1}_{y_c} = \vec{1}_{r_c} \times \vec{d}_1 \\ \vec{1}_{r_c} &\equiv \vec{1} - \vec{1}_{r_c} \vec{1}_{r_c}\end{aligned}$$

$$Z_0 = \left[\frac{\mu_0}{\epsilon_0} \right]^{\frac{1}{2}}, \quad c = [\mu_0 \epsilon_0]^{\frac{1}{2}}$$

$\mu_0 \equiv$ permeability of free space (7.4)

$\epsilon_0 \equiv$ permittivity of free space

$s = \Omega + j\omega \equiv$ complex frequency or Laplace-transform variable (two-sided)

The two pattern functions \vec{d}_1 and \vec{d}_2 contain the information concerning polarization and variation with angles θ_c and ϕ_c .

One can define a power pattern in the far field [4] (related to the Poynting vector)

$$\begin{aligned}\vec{P} &= \vec{d}_1 \times \vec{d}_2 = \vec{d}_1 \times [\vec{1}_{r_c} \times \vec{d}_1] = \vec{1}_{r_c} [\vec{d}_1 \cdot \vec{d}_1] \\ &= P_{r_c} \vec{1}_{r_c} \\ P_{r_c} &= |\vec{d}_1|^2 = 2[1 + \vec{1}_{z_c} \cdot \vec{1}_{r_c}] - [\vec{1}_{x_c} \cdot \vec{1}_{r_c}]^2 - [\vec{1}_{y_c} \cdot \vec{1}_{r_c}]^2 \\ &= 2[1 + \cos(\theta_c)] - \sin^2(\theta_c) \cos^2(\phi_c) - \sin^2(\theta_c) \sin^2(\phi_c) \\ &= 2[1 + \cos(\theta_c)] - \sin^2(\theta_c) \\ &= 1 + 2\cos(\theta_c) + \cos^2(\theta_c) \\ &= [1 + \cos(\theta_c)]\end{aligned} \tag{7.5}$$

This is known as a cardioid pattern. It has rotation symmetry (O_2) with respect to the z_c axis. One can normalize this via

$$\begin{aligned}P_{avg} &= \frac{1}{4\pi} \int_0^\pi \int_0^{2\pi} [1 + \cos(\theta_c)]^2 \sin(\theta_c) d\theta_c d\phi_c \\ &= \frac{1}{2} \int_0^\pi [1 + \cos(\theta_c)]^2 \sin(\theta_c) d\theta_c \\ &= \frac{1}{2} \int_{-1}^1 [1 + v]^2 dv \quad (v = \cos(\theta_c))\end{aligned} \tag{7.6}$$

$$= \frac{1}{2} \frac{[1+\nu]^3}{3} \Big|_{-1}^1 = \frac{4}{3}$$

the 4π normalization being from the area of the unit sphere. So the directivity of this antenna is

$$\frac{P_c}{P_{avg}} = \frac{3}{4} [1 + \cos(\theta_c)]^2 \quad (7.7)$$

Considering the vector field components the situation is not quite so symmetrical. From (7.4) the two pattern functions characterize the angular dependence of the fields, and can be used to characterize the two polarization modes of the antenna, since the two polarizations correspond to an interchange of the roles of the electric and magnetic fields, or a rotation by $\pi/2$ (90°) around the z_c axis (for this kind of antenna).

The first pattern (for the electric field) which we can call the vertical mode is described by

$$\begin{aligned} \vec{d}_1 &= \vec{1}_{x_c} - \vec{1}_{r_c} \vec{1}_{r_c} \cdot \vec{1}_{x_c} - \vec{1}_{r_c} \times \vec{1}_{y_c} \\ &= \vec{1}_{x_c} - [\vec{1}_{x_c} \sin(\theta_c) \cos(\phi_c) + \vec{1}_{y_c} \sin(\theta_c) \sin(\phi_c) + \vec{1}_{z_c} \cos(\theta_c)] \sin(\theta_c) \cos(\phi_c) \\ &\quad - \vec{1}_{z_c} \sin(\theta_c) \cos(\phi_c) + \vec{1}_{x_c} \cos(\theta_c) \\ &= \vec{1}_{x_c} [1 + \cos(\theta_c) - \sin^2(\theta_c) \cos^2(\phi_c)] - \vec{1}_{y_c} \sin^2(\theta_c) \sin(\phi_c) \cos(\phi_c) \\ &\quad - \vec{1}_{z_c} \sin(\theta_c) \cos(\phi_c) [1 + \cos(\theta_c)] \end{aligned} \quad (7.8)$$

On the $x_c = 0$ plane we have

$$\begin{aligned} \phi_c &= \pm \frac{\pi}{2} \\ \vec{d}_1 &= \vec{1}_{x_c} [1 + \cos(\theta_c)] \end{aligned} \quad (7.9)$$

Similarly on the $y_c = 0$ plane we have

$$\begin{aligned} \phi_c &= 0, \pi \\ \vec{d}_1 &= \vec{1}_{x_c} \cos(\theta_c) [1 + \cos(\theta_c)] - \text{sign}(x_c) \vec{1}_{z_c} \sin(\theta_c) [1 + \cos(\theta_c)] \\ &= - \vec{1}_{z_c} [1 + \cos(\theta_c)] \text{sign}(x_c) \end{aligned} \quad (7.10)$$

This shows the $1 + \cos(\theta_c)$ pattern in both E and H planes for the vertical mode, with polarization in the vertical direction.

The second pattern (for the magnetic field) which we can call the horizontal mode is described by

$$\begin{aligned}
\vec{d}_2 &= \vec{1}_{r_c} \times \vec{1}_{x_c} + \vec{1}_{y_c} - \vec{1}_{r_c} \vec{1}_{r_c} \cdot \vec{1}_y \\
&= -\vec{1}_{z_c} \sin(\theta_c) \sin(\phi_c) + \vec{1}_{y_c} \cos(\theta_c) + \vec{1}_{y_c} \\
&\quad - [\vec{1}_{x_c} \sin(\theta_c) \cos(\phi_c) + \vec{1}_{y_c} \sin(\theta_c) \sin(\phi_c) + \vec{1}_{z_c} \cos(\theta_c)] \sin(\theta_c) \sin(\phi_c) \\
&= -\vec{1}_{x_c} \sin^2(\theta_c) \sin(\phi_c) \cos(\phi_c) + \vec{1}_{y_c} [1 + \cos(\theta_c) - \sin^2(\theta_c) \sin^2(\phi_c)] \\
&\quad - \vec{1}_{z_c} [1 + \cos(\theta_c)] \sin(\theta_c) \sin(\phi_c)
\end{aligned} \tag{7.11}$$

On the $x_c = 0$ plane we have

$$\begin{aligned}
\phi_c &= \pm \frac{\pi}{2} \\
\vec{d}_2 &= \vec{1}_{y_c} \cos(\theta_c) [1 + \cos(\theta_c)] - \text{sign}(y_c) \vec{1}_{z_c} \sin(\theta_c) [1 + \cos(\theta_c)] \\
&= \vec{1}_{\theta_c} [1 + \cos(\theta_c)] \text{sign}(y_c)
\end{aligned} \tag{7.12}$$

On the $y_c = 0$ plane we have

$$\begin{aligned}
\phi_c &= 0, \pi \\
\vec{d}_2 &= \vec{1}_{y_c} [1 + \cos(\theta_c)]
\end{aligned} \tag{7.13}$$

Again we have the $1 + \cos(\theta_c)$ pattern in both E and H planes for the horizontal mode with polarization in the horizontal direction.

With these results let us return to the geometry discussed in the previous section (Section 6). As in Fig. 6.1 we have a symmetry plane S_0 which is nearly horizontal and is perpendicular to a vertical plane S_y . Specifically let z_c , the axis of our combined-dipole pattern lie on the intersection of S_0 with S_y and point toward the target site. By appropriate choice of x_c and y_c both S_0 and S_y can be symmetry planes for the incident fields.

Recognizing the two pattern functions as describing the two polarization modes we can choose

$$\begin{aligned}
 y_c &= -y \quad , \quad \vec{1}_{y_c} = -\vec{1}_y \\
 x_c \text{ and } z_c &\text{ in } S_y \text{ plane}
 \end{aligned}
 \tag{7.14}$$

Here x_c is a nearly vertical coordinate and z_c is a nearly horizontal coordinate; both can be described in terms of x and y as

$$\begin{aligned}
 z_c &= z \cos(\psi_0) + x \sin(\psi_0) \\
 x_c &= x \cos(\psi_0) - z \sin(\psi_0) \\
 \vec{1}_{z_c} &= \vec{1}_z \cos(\psi_0) + \vec{1}_x \sin(\psi_0) \\
 \vec{1}_{x_c} &= \vec{1}_x \cos(\psi_0) - \vec{1}_z \sin(\psi_0)
 \end{aligned}
 \tag{7.15}$$

With these definitions, one can compute \vec{d}_1 for vertical mode and \vec{d}_2 for horizontal mode in terms of (x, y, z) or (x_c, y_c, z_c) coordinates.

On the S_y plane (a symmetry plane for such fields), and hence for $y = 0$ on the target site, the polarization is purely horizontal and vertical as discussed in Section 5. For positions away from S_y the polarization is not ideal, but approaches the ideal case for small ψ_0 . In any event the polarization can be calculated from the formulas given previously.

8. Concluding Remarks

Using symmetry concepts one can attempt to get the polarizations as purely vertical and horizontal as possible. If desired, one can then correct deviations from the ideal by rotating the scattering dyadic in a computer based on the actual calculated and/or measured incident-field orientations at each position of interest on the target site.

As discussed in Section 3, O_2 antennas with a vertical symmetry axis provide purely vertical and horizontal polarization over all of S_e . However, such antennas have patterns independent of azimuth ϕ , implying that they transmit to (and receive from) positions away from the target site (negative x). This introduces undesirable clutter into the SAR image. So some compromise of this pattern is appropriate. One can use the concept of partial symmetry discussed in Section 1 to help here. By placing some large scattering surface some distance behind the antennas (negative x), one can make the signal from the target reach the antennas some clear time t_c before this signal scatters from the surface back to the antennas. If the target-scattered pulse width (of interest) is less than t_c then in this time window the O_2 symmetry analysis is still correct. The return of the direct scattering surface also needs to be placed at a time which does not interfere with the desired target-scattered signal. Additionally this rear scattering surface can be made absorptive.

More generally, limiting patterns to some range of ϕ requires one to consider less symmetrical antennas. Symmetry planes as discussed in Sections 5 through 7 are still appropriate for this purpose. Many kinds of antennas can be constructed with such symmetry planes. How pure are the polarizations away from the symmetry planes will depend on the design specifics. Note that deviations from the ideal are frequency dependent, generally different for every frequency in the radiated and scattered pulses.

References

1. C. E. Baum, Some Characteristics of Electric and Magnetic Dipole Antennas for Radiating Transient Pulses, Sensor and Simulation Note 125, January 1971.
2. J. S. Yu, C.-L. J. Chen, and C. E. Baum, Multipole Radiations: Formulation and Evaluation for Small EMP Simulators, Sensor and Simulation Note 243, July 1978.
3. E. G. Farr and J. S. Hostra, An Incident Field Sensor for EMP Measurements, Sensor and Simulation Note 319, November 1989; IEEE Trans. EMC, 1991, pp. 105-112.
4. C. E. Baum, General Properties of Antennas, Sensor and Simulation Note 330, July 1991.
5. F. M. Tesche, The P x M Antenna and Applications to Radiated Field Testing of Electrical Systems, Part 1: Theory and Numerical Simulations, Sensor and Simulation Note 407, July 1997.
6. F. M. Tesche, T. Karlsson, and S. Garmland, The P x M Antenna and Applications to Radiated Field Testing of Electrical Systems, Part 2: Experimental Considerations, Sensor and Simulation Note 409, August 1997.
7. C. E. Baum, Symmetry in Electromagnetic Scattering as a Target Discriminant, Interaction Note 523, October 1996; Wideband Interferometric Sensing and Imaging Polarimetry, H. Mott and W. Boerner (eds.), Proc. SPIE, Vol. 3120, 1997, pp. 295-307.
8. L. Carin, R. Kapoor, and C. E. Baum, Polarimetric SAR Imaging of Buried landmines, IEEE Trans. Geoscience and Remote Sensing, 1998, pp. 1985-1988.
9. C. E. Baum, Electromagnetic Sensors and Measurement Techniques, pp. 73-144, in J. E. Thompson and L. H. Luessen, *Fast Electrical and Optical Measurements*, Martinus Nijhoff, Dordrecht, 1986.
10. C. E. Baum and H. N. Kritikos, Symmetry in Electromagnetics, ch. 1, pp. 1-90, in C. E. Baum and H. N. Kritikos (eds.), *Electromagnetic Symmetry*, Taylor & Francis, 1995.
11. C. E. Baum, Symmetry and Transforms of Waveforms and Waveform Spectra in Target identification, ch. 7, pp. 309-343, in C. E. Baum and H. N. Kritikos (eds.), *Electromagnetic Symmetry*, Taylor & Francis, 1995.
12. J. McCorkle, V. Sabio, R. Kapoor, and N. Nandhakumar, Transient Synthetic Aperture Radar and the Extraction of Anisotropic and Natural Frequency information, ch. 12, pp. 375-430, in C. E. Baum (ed.), *Detection and Identification of Visually Obscured Targets*, Taylor & Francis, 1998.

